Electric Supplementary Information

Silver(I)-Induced Higher-Ordered Structure Based on Planar Chiral Tetrasubstituted [2.2]Paracyclophane

Masayuki Gon[a], Yasuhiro Morisaki[a,b], and Yoshiki Chujo*[,a]

[a] Department of Polymer Chemistry, Graduate School of Engineering, Kyoto University, Nishikyo-ku, Katsura, Kyoto 615-8510, Japan.

[b] Present address: Department of Applied Chemistry for Environment, School of Science and Technology, Kwansei Gakuin University, 2-1 Gakuen, Sanda, Hyogo 669-1337 Japan.

E-mail: chujo@chujo.synchem.kyoto-u.ac.jp

Contents:

General

^{1}H and ^{13}C NMR spectra were recorded on JEOL EX400 and AL400 instruments at 400 and 100 MHz, respectively. Samples were analyzed in and CD_2Cl_2. Analytical thin layer chromatography (TLC) was performed with silica gel 60 Merck F254 plates. Column chromatography was performed with Wakogel® C-300 silica gel and aluminium oxide 90 active basic (0.063-0.200 mm, pH = 8.5-10.5). High-resolution mass (HRMS) spectrometry was performed at the Technical Support Office (Department of Synthetic Chemistry and Biological Chemistry, Graduate School of Engineering, Kyoto University), and the HRMS spectra were obtained on a Thermo Fisher Scientific EXACTIVE spectrometer for electrospray ionization (ESI). Recyclable preparative high-performance liquid chromatography (HPLC) was carried out on a Japan Analytical Industry Co. Ltd., Model LC918R (JAIGEL-1H and 2H columns) using $CHCl_3$ as an eluent. UV–vis spectra were recorded on a SHIMADZU UV-3600 spectrophotometer, and samples were analyzed in CH_2Cl_2 at room temperature. Fluorescence emission spectra were recorded on a HORIBA JOBIN YVON Fluoromax-4 spectrofluorometer, and samples were analyzed in CH_2Cl_2 at room temperature. Specific rotations ($[\alpha]^{t}_{D}$) were measured with a HORIBA SEPA-500 polarimeter. Circular dichroism (CD) spectra were recorded on a JASCO J-820 spectropolarimeter with CH_2Cl_2 as a solvent at room temperature. Circularly polarized luminescence (CPL) spectra were recorded on a JASCO CPL-200S with CH_2Cl_2 as a solvent at room temperature. The PL lifetime measurement was performed on a Horiba FluoreCube spectrofluorometer system; excitation was carried out using a UV diode laser (NanoLED 375 nm). Elemental analyses were performed at the Microanalytical Center of Kyoto University.

Materials

Commercially available compounds used without purification:

2-Iodo-pyridine (**1**) (Tokyo Chemical Industry Co, Ltd.)

$Pd_2(dba)_3$ (dba = dibenzylideneacetone) (Tokyo Chemical Industry Co, Ltd.)

1,1'-bis(diphenylphosphino)ferrocene (dppf) (Tokyo Chemical Industry Co, Ltd.)

CuI (Wako Pure Chemical Industries, Ltd.)

K_2CO_3 (Wako Pure Chemical Industries, Ltd.)

AgOTf (Silver(I) trifluoromethanesulfonate) (Strem Chemicals Inc.)

Commercially available solvents:

CH_2Cl_2 (deoxidized grade, Wako Pure Chemical Industries, Ltd.) used without purification.

THF (Wako Pure Chemical Industries, Ltd.) and Et_3N (Kanto Chemical Co., Inc.) purified by passage through solvent purification columns under Ar pressure.[1]

Compounds prepared as described in the literatures:

2-Bromo-6-(phenylethynyl)pyridine (**2**)[2]

(S_p)- and (R_p)-4,7,12,15-Tetraethynyl[2.2]paracyclophane ((S_p)- and (R_p)-**Cp**)[3]

Synthetic Procedures and Characterization

Synthesis of (S_p)-N-H

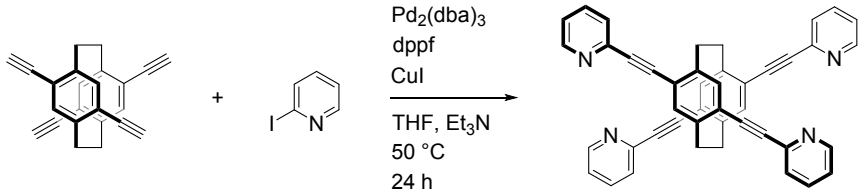

(S_p)-**Cp** **1** (S_p)-**N-H**, 64%

A mixture of (S_p)-**Cp** (20.0 mg, 0.0657 mmol), 2-iodopyridine (**1**) (59.3 mg, 0.289 mmol), $Pd_2(dba)_3$ (6.0 mg, 0.00657 mmol), dppf (7.3 mg, 0.0131 mmol), CuI (2.5 mg, 0.0131 mmol), THF (2 mL) and Et_3N (2 mL) was placed in a round-bottom flask equipped with magnetic stirring bar. After degassing the reaction mixture several times, the reaction was carried out at room temperature for 24 h. After the reaction, precipitates were removed by filtration, and the solvent was evaporated. The residue was semi-purified by flash column chromatography on basic (pH = 8.5-10.5) Al_2O_3 (EtOAc as an eluent) and recrystallization from CH_2Cl_2 and Hexane (good and poor solvent, respectively) to afford (S_p)-**N-H** (25.7 mg, 0.0419 mmol, 64%) as a colorless crystal.

R_f = 0.23 (EtOAc/CH_2Cl_2 = 1/1 v/v). ^{1}H NMR (CD_2Cl_2, 400 MHz) δ 3.16-3.24 (m, 4H), 3.61-3.69 (m, 4H), 7.25 (s, 4H), 7.31 (ddd, J = 1.4, 4.8, 7.6 Hz, 4H), 7.65 (td, J = 1.2, 7.8 Hz, 4H), 7.75 (dt, J = 1.8, 7.7 Hz, 4H), 8.67 (ddd, J = 0.96, 1.7, 4.8 Hz, 4H) ppm; ^{13}C NMR (CD_2Cl_2, 100 MHz) δ 33.2, 88.5, 94.9, 123.4, 125.3, 128.0, 135.5, 136.6, 143.2, 143.9, 150.6 ppm. HRMS (ESI) calcd. for $C_{44}H_{29}N_4$ $[M+H]^+$: 613.2387, found: 613.2364. Elemental analysis calcd. for $C_{44}H_{28}N_4$: C 86.25 H 4.61 N 9.14, found: C 86.22 H 4.57 N 9.09.

(R_p)-**N** and was obtained by the same procedure in 86% isolated yield.

(S_p)-**N**: $[\alpha]^{23}_D$ = −96.4 (c 0.5, CH_2Cl_2). (R_p)-**N**: $[\alpha]^{23}_D$ = +97.7 (c 0.5, CH_2Cl_2).

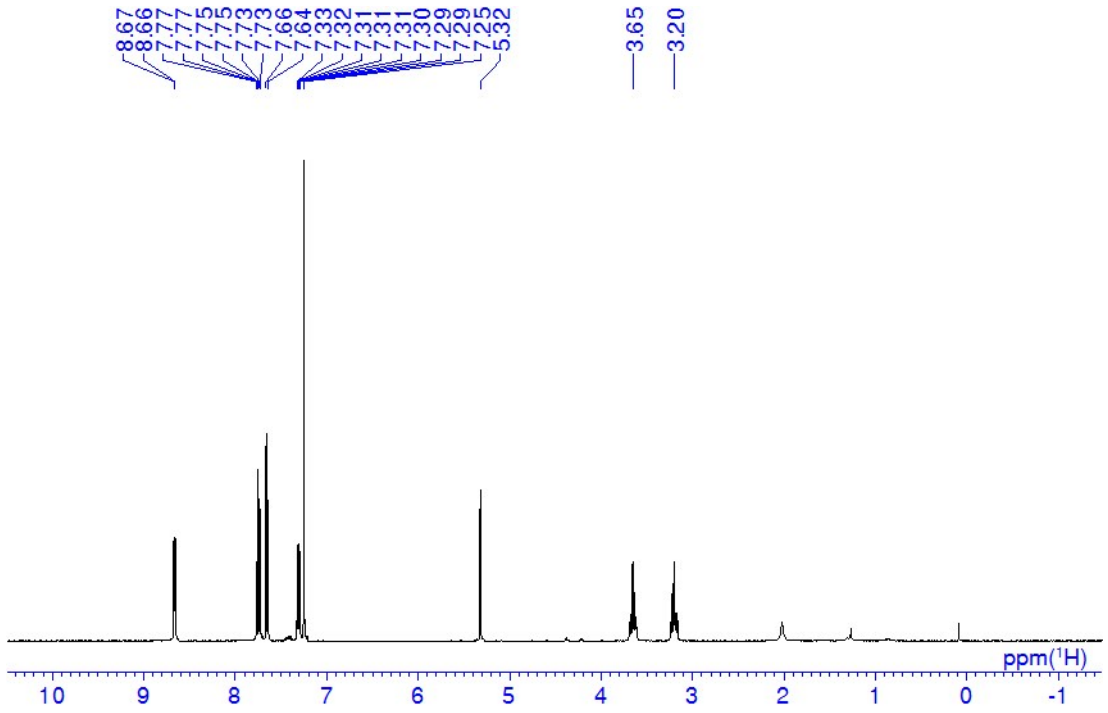

Figure S1. ^{1}H NMR spectrum of (S_p)-**N-H** in CD_2Cl_2.

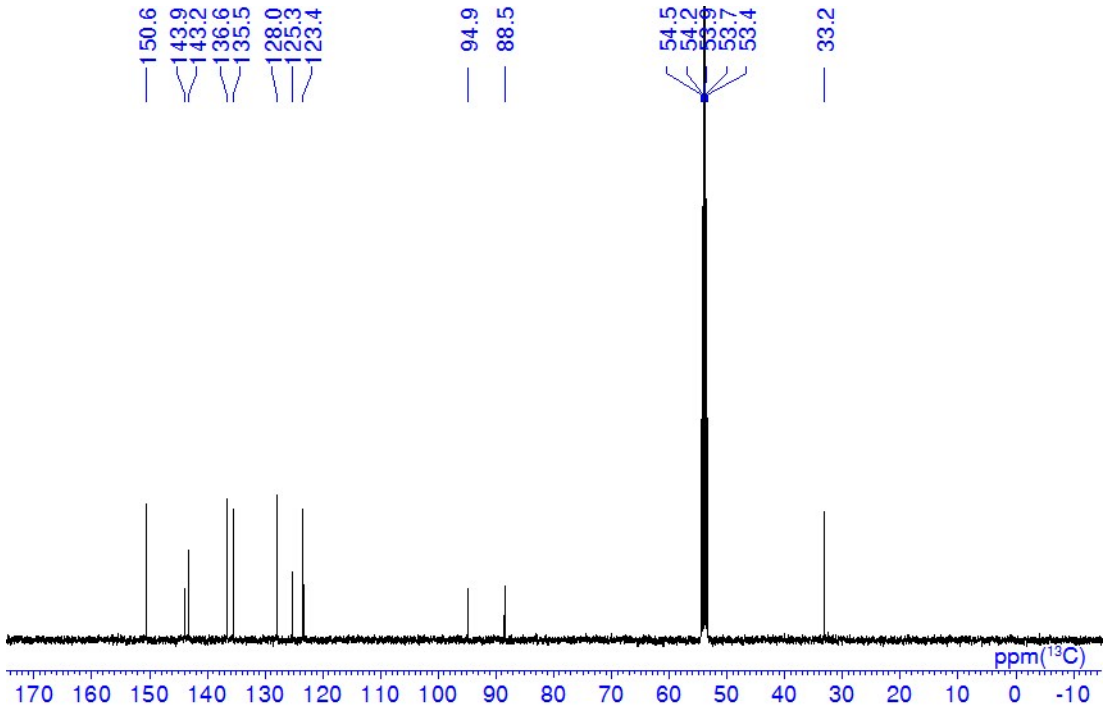

Figure S2. ^{13}C NMR spectrum of (S_p)-**N-H** in CD_2Cl_2.

Synthesis of (S_p)-N-Ph

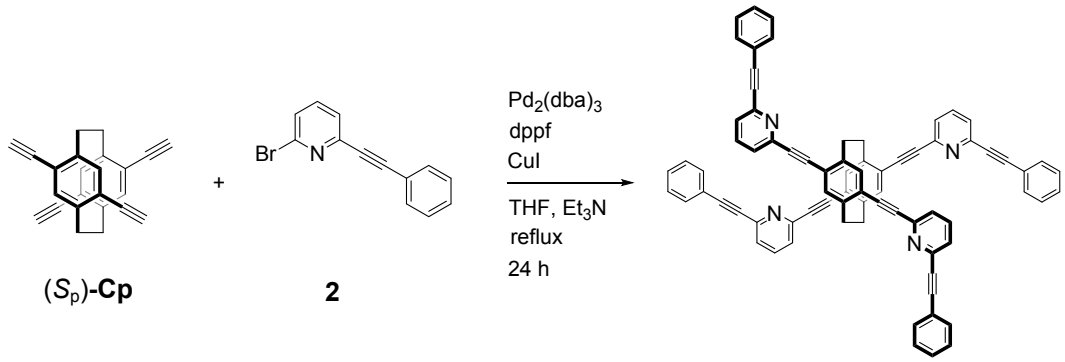

(S_p)-**Cp** **2** (S_p)-**N-Ph**, 15%

A mixture of (S_p)-**Cp** (30.0 mg, 0.0986 mmol), 2-bromo-6-(phenylethynyl)pyridine (**2**) (127 mg, 0.493 mmol), $Pd_2(dba)_3$ (9.0 mg, 0.00986 mmol), dppf (10.9 mg, 0.0197 mmol), CuI (3.8 mg, 0.0197 mmol), THF (3 mL) and Et_3N (3 mL) was placed in a round-bottom flask equipped with magnetic stirring bar. After degassing the reaction mixture several times, the reaction was carried out at reflux condition for 24 h. After the reaction, precipitates were removed by filtration, and the solvent was evaporated. The residue was semi-purified by flash column chromatography on SiO_2 (CH_2Cl_2/EtOAc = 9/1 v/v as an eluent). Further purification was carried out by HPLC with $CHCl_3$ and flash column chromatography on basic (pH = 8.5-10.5) Al_2O_3 (CH_2Cl_2/EtOAc = 19/1 v/v as an eluent). The purified sample was collected by lyophilization with benzene to afford (S_p)-**N-Ph** (14.6 mg, 0.0144 mmol, 15%) as a colorless powder.

R_f = 0.23 (CH_2Cl_2). ^{1}H NMR (CD_2Cl_2, 400 MHz) δ 3.21-3.29 (m, 4H), 3.66-3.74 (m, 4H), 7.32 (s, 4H), 7.39-7.44 (m, 12H), 7.51 (dd, J = 0.72, 7.6 Hz, 4H), 7.61-7.66 (m, 8H), 7.72 (dd, J = 0.72, 7.8 Hz, 4H), 7.78 (t, J = 7.8 Hz, 4H), ppm; ^{13}C NMR (CD_2Cl_2, 100 MHz) δ 33.0, 88.9, 88.9, 89.6, 94.6, 122.4, 125.4, 126.9, 127.4, 128.9, 129.6, 132.4, 135.8, 137.1, 143.2, 144.1, 144.2 ppm. HRMS (ESI) calcd. for $C_{76}H_{45}N_4$ $[M+H]^+$: 1013.3639, found: 1013.3624. Elemental analysis calcd. for $C_{76}H_{44}N_4$: C 90.09 H 4.38 N 5.53, found: C 89.82 H 4.53 N 5.51.

(R_p)-**N-Ph** and was obtained by the same procedure in 21% isolated yield.

(S_p)-**N-Ph**: $[\alpha]^{23}_D$ = +16.8 (c 0.5, CH_2Cl_2). (R_p)-**N-Ph**: $[\alpha]^{23}_D$ = −16.5 (c 0.5, CH_2Cl_2).

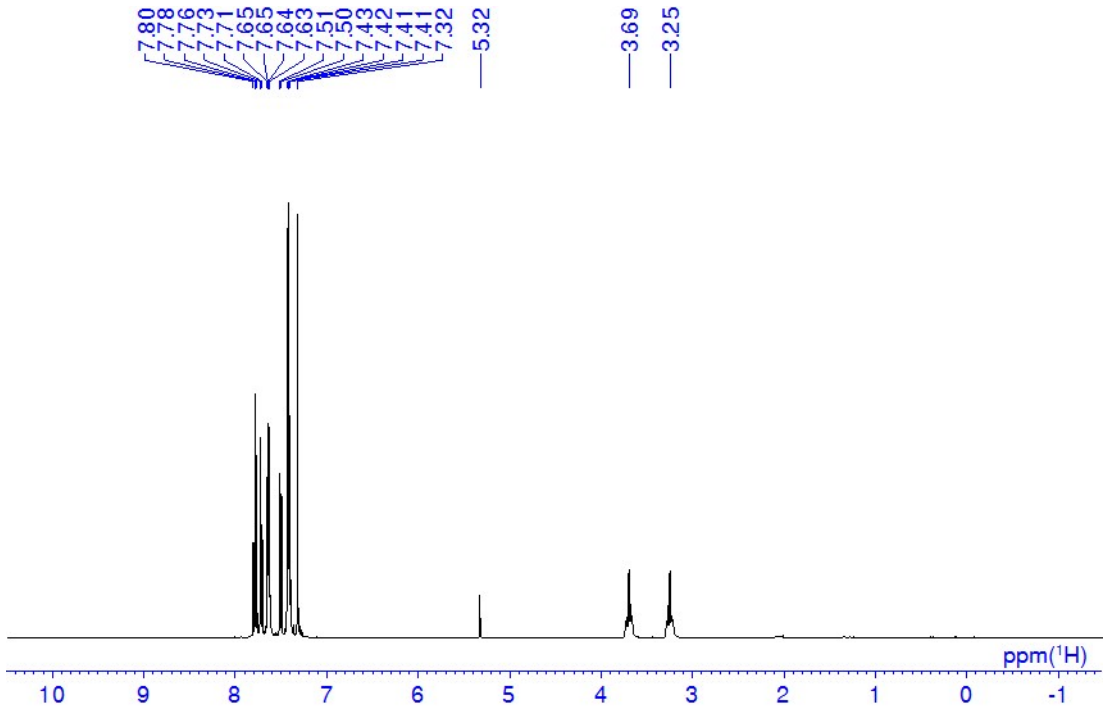

Figure S3. ^{1}H NMR spectrum of (S_p)-**N-Ph** in CD_2Cl_2.

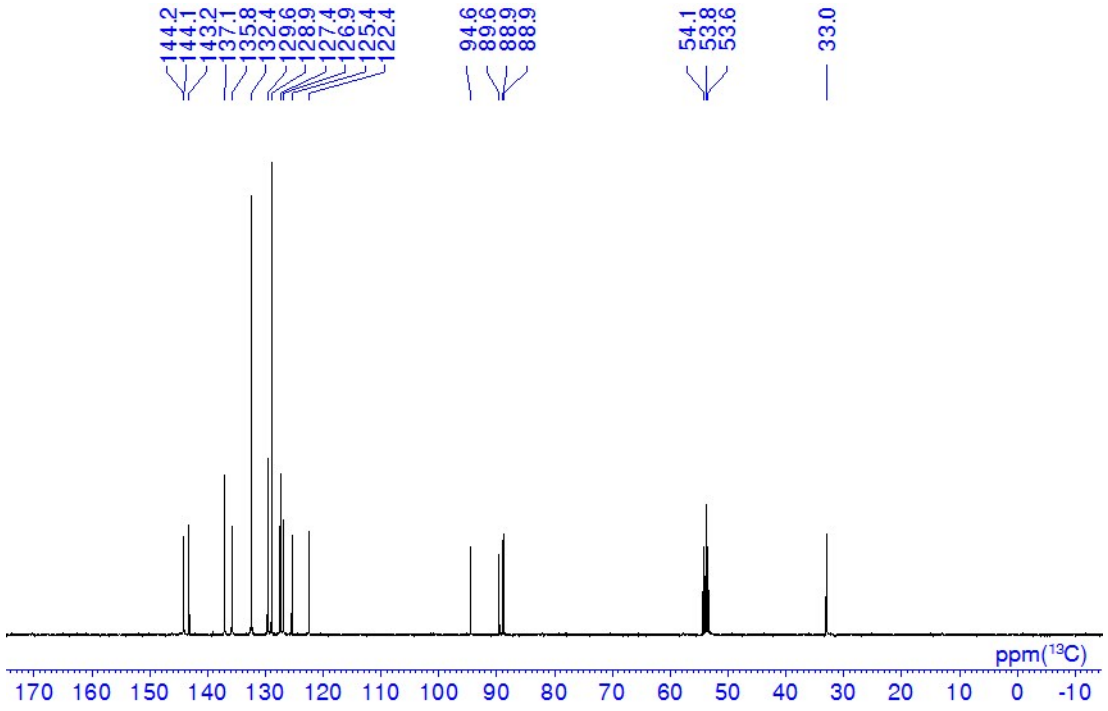

Figure S4. ^{13}C NMR spectrum of (S_p)-**N-Ph** in CD_2Cl_2.

Ag Coordinate Compounds

The preparation methods of the Ag(I) coordinate compounds, (S_p)-**N-H-Ag** and (S_p)-**N-Ph-Ag** are shown here. Ag(I) coordination was confirmed by ^{1}H and ^{13}C NMR spectra. The difference of solubility between starting compounds and obtained compounds supports the Ag(I) coordination. Although Ag(I) coordination was also confirmed by HRMS spectra, *trans*-*N*-*N*-Ag(I) coordinate compounds having two coordination sites are usually detected as mono-coordinate compounds in HRMS spectra.

Preparation of (S_p)-N-H-Ag

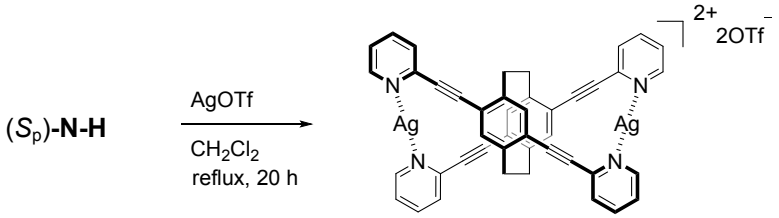

(S_p)-**N-H-Ag**, 88%

A mixture of (S_p)-**N-H** (10.0 mg, 0.0163 mmol) and AgOTf (16.8 mg, 0.0652 mmol) was placed in a round-bottom flask equipped with magnetic stirring bar. After degassing the reaction mixture several times, CH_2Cl_2 (1.0 mL) were added to the mixture. The reaction was carried out at reflux temperature for 14 h. After the reaction, all CH_2Cl_2 were dried over in the same flask. The residue was dissolved in CH_2Cl_2 and filtered to remove excess AgOTf. After the solvent of filtrate was evaporated, the residue was dissolved in CH_3CN and filtered to remove unreacted (S_p)-**N-H**. After the solvent of filtrate was evaporated, repreticipation with CH_2Cl_2 and hexane (good and poor solvent, respectively) was carried out to afford (S_p)-**N-H-Ag** (16.1 mg, 0.0143 mmol, 88%) as a light yellow solid. (S_p)-**N-H** was not dissolved in CH_3CN, but (S_p)-**N-H-Ag** was dissolved in CH_3CN.

^{1}H NMR (CD_2Cl_2, 400 MHz) δ 3.05-3.14 (m, 4H), 3.49-3.57 (m, 4H), 7.30 (s, 4H), 7.60 (ddd, J = 7.6 5.5, 1.3 Hz, 4H), 7.82 (d, J = 7.6 Hz, 4H), 8.00 (dt, J = 7.8, 1.6 Hz, 4H), 9.07 (d, J = 4.7 Hz, 4H) ppm; ^{13}C NMR (CD_2Cl_2, 100 MHz) δ 32.8, 91.9, 94.2, 121.1 (q, J = 320 Hz), 125.1, 125.4. 129.2, 135.4, 139.7, 143.5. 143.8, 153.8 ppm. HRMS (ESI) calcd. for $C_{44}H_{28}N_4Ag$ [M-Ag(OTf)$_2$]$^+$: 719.1359, found: 719.1346.

(R_p)-**N-Ag** was obtained by the same procedure in isolated 91% yield.

(S_p)-**N-Ag**: $[\alpha]^{23}_D$ = −33.4 (*c* 0.5, CH_2Cl_2). (R_p)-**N-Ag**: $[\alpha]^{23}_D$ = +36.2 (*c* 0.5, CH_2Cl_2).

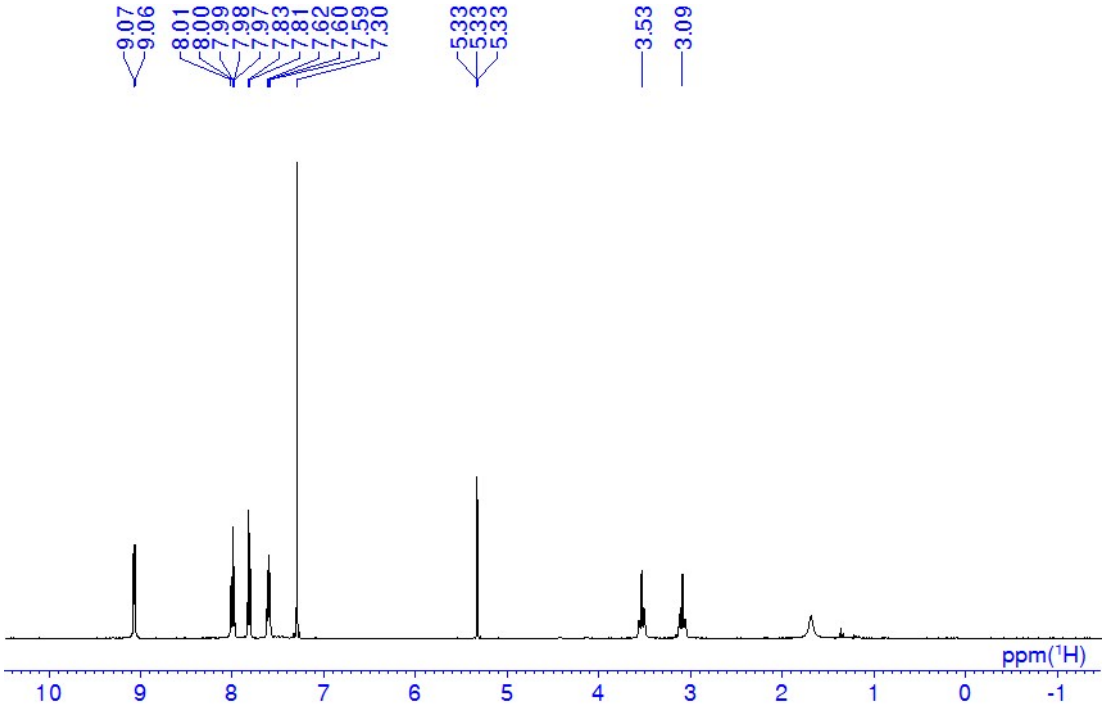

Figure S5. ^{1}H NMR spectrum of (S_p)-**N-H-Ag** in CD_2Cl_2.

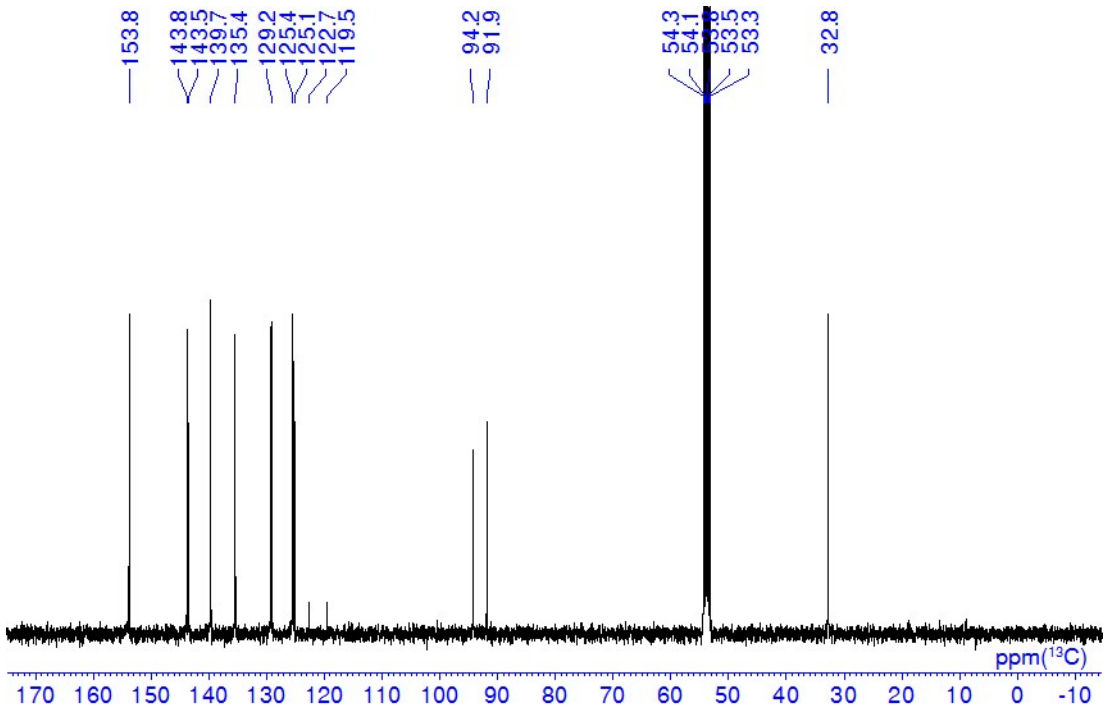

Figure S6. ^{13}C NMR spectrum of (S_p)-**N-H-Ag** in CD_2Cl_2.

Preparation of (S_p)-N-Ph-Ag

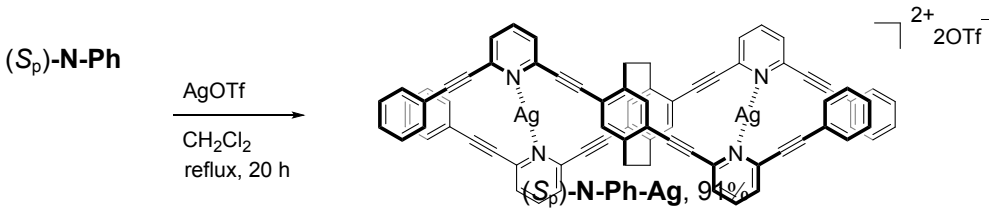

A mixture of (S_p)-**N-Ph** (10.0 mg, 0.00987 mmol) and AgOTf (25.4 mg, 0.0987 mmol) was placed in a round-bottom flask equipped with magnetic stirring bar. After degassing the reaction mixture several times, CH_2Cl_2 (1.0 mL) were added to the mixture. The reaction was carried out at reflux temperature for 20 h. After the reaction, all CH_2Cl_2 were dried over in the same flask. The residue was dissolved in CH_2Cl_2 and filtered to remove excess AgOTf. After the solvent of filtrate was evaporated, the residue was dissolved in MeOH and filtered to remove unreacted (S_p)-**N-Ph**. After the solvent of filtrate was evaporated, repreticipation with CH_2Cl_2 and hexane (good and poor solvent, respectively) was carried out to afford (S_p)-**N-Ph-Ag** (13.7 mg, 0.00897 mmol, 91%) as a light yellow solid. (S_p)-**N-Ph** was not dissolved in CH_3OH, but (S_p)-**N-Ph-Ag** was dissolved in CH_3OH.

^{1}H NMR (CD_2Cl_2, 400 MHz) δ 3.12-3.20 (m, 4H), 3.56-3.64 (m, 4H), 7.25-7.29 (m, 8H), 7.32-7.35 (m, 8H), 7.39-7.44 (m, 4H), 7.45 (s, 4H), 7.80 (dd, J = 7.8, 0.96 Hz, 4H), 7.90 (dd, J = 7.8, 0.96 Hz, 4H), 8.13 (t, J = 7.8 Hz, 4H) ppm; ^{13}C NMR (CD_2Cl_2, 100 MHz) δ 33.0, 87.3, 93.0, 93.7, 95.6, 120.4, 124.9, 128.4, 128.5, 128.7, 130.6, 132.6, 135.8, 140.7, 143.9, 144.3, 145.1 ppm (quartet CF_3 peaks of trifluoromethanesulfonate are not detected). HRMS (ESI) calcd. for $C_{76}H_{44}N_4Ag$ $[M\text{-}Ag(OTf)_2]^+$: 1119.2611, found: 1119.2607.

(R_p)-**N-Ph-Ag** was obtained by the same procedure in 93% isolated yield.

(S_p)-**N-Ph-Ag**: $[\alpha]^{23}_D$ = +172.0 (c 0.5, CH_2Cl_2). (R_p)-**N-Ph-Ag**: $[\alpha]^{23}_D$ = −167.0 (c 0.5, CH_2Cl_2).

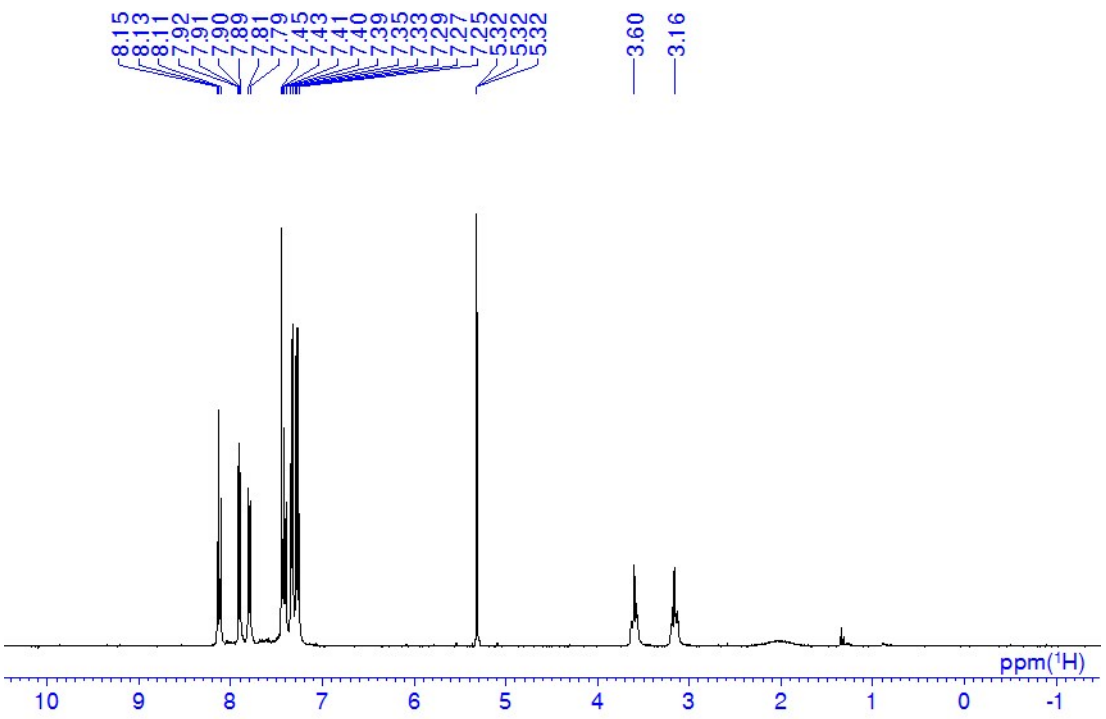

Figure S7. ^{1}H NMR spectrum of (S_p)-**N-Ph-Ag** in CD_2Cl_2.

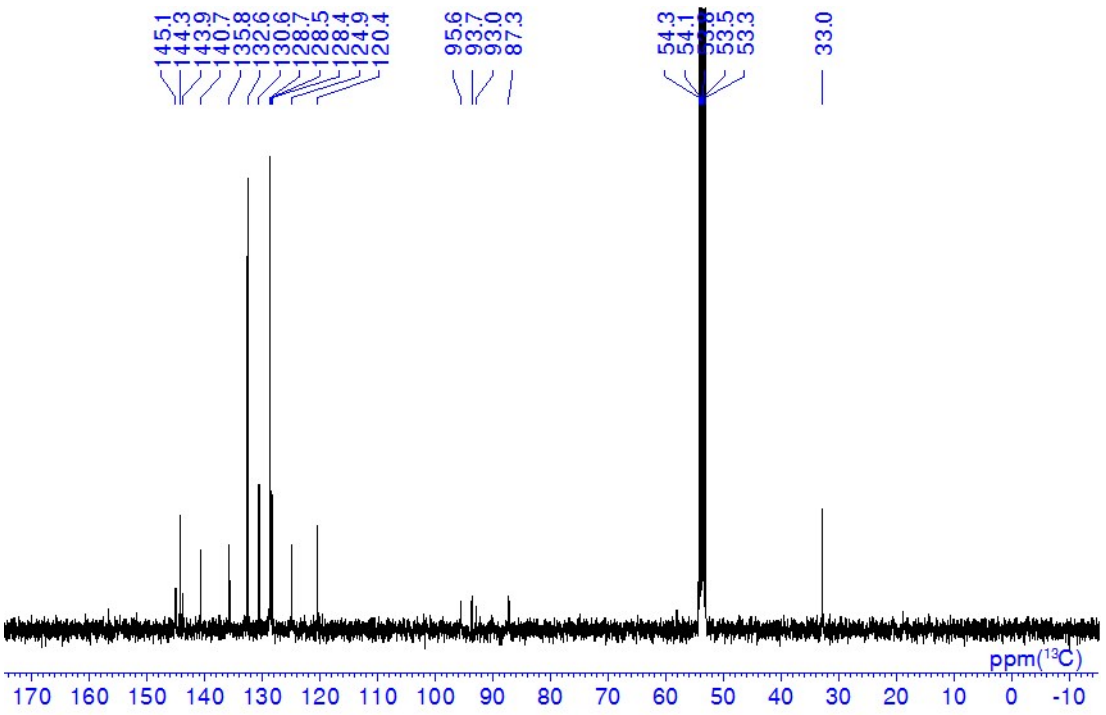

Figure S8. ^{13}C NMR spectrum of (S_p)-**N-Ph-Ag** in CD_2Cl_2.

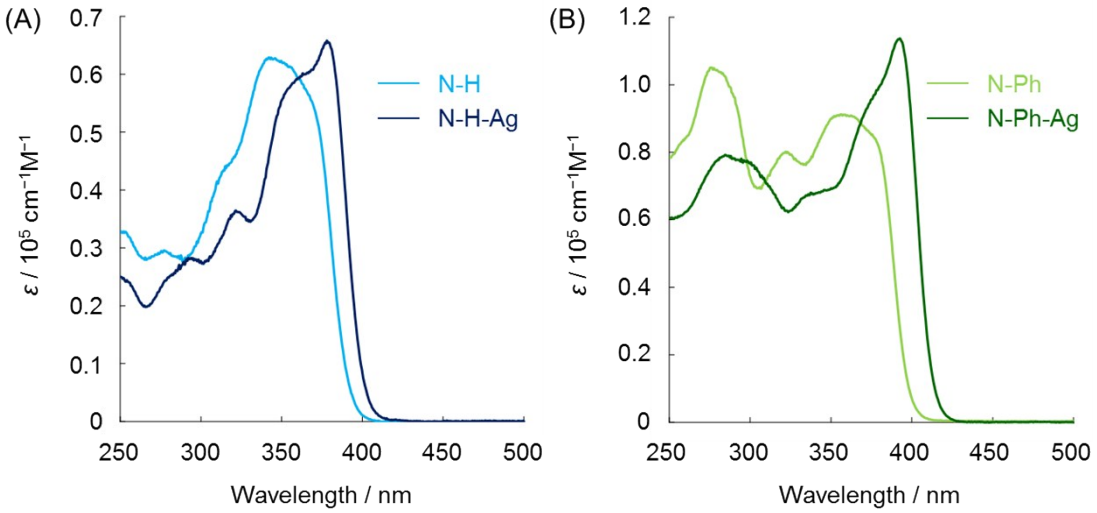

Figure S9. UV–vis absorption spectra of (A) **N-H** and **N-H-Ag**, (B) **N-Ph** and **N-Ph-Ag** in dilute CH_2Cl_2 (1.0×10^{-5} M).

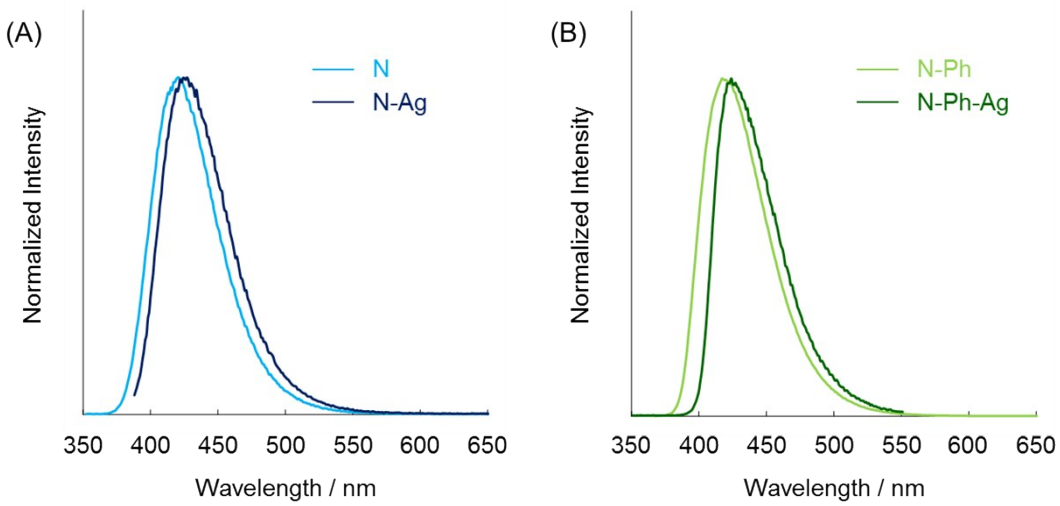

Figure S10. PL spectra of (A) **N-H** and **N-H-Ag**, (B) **N-Ph** and **N-Ph-Ag** in dilute CH_2Cl_2 (1.0×10^{-5} M). Excitation was carried out at the peak top of UV–vis absorption spectra.

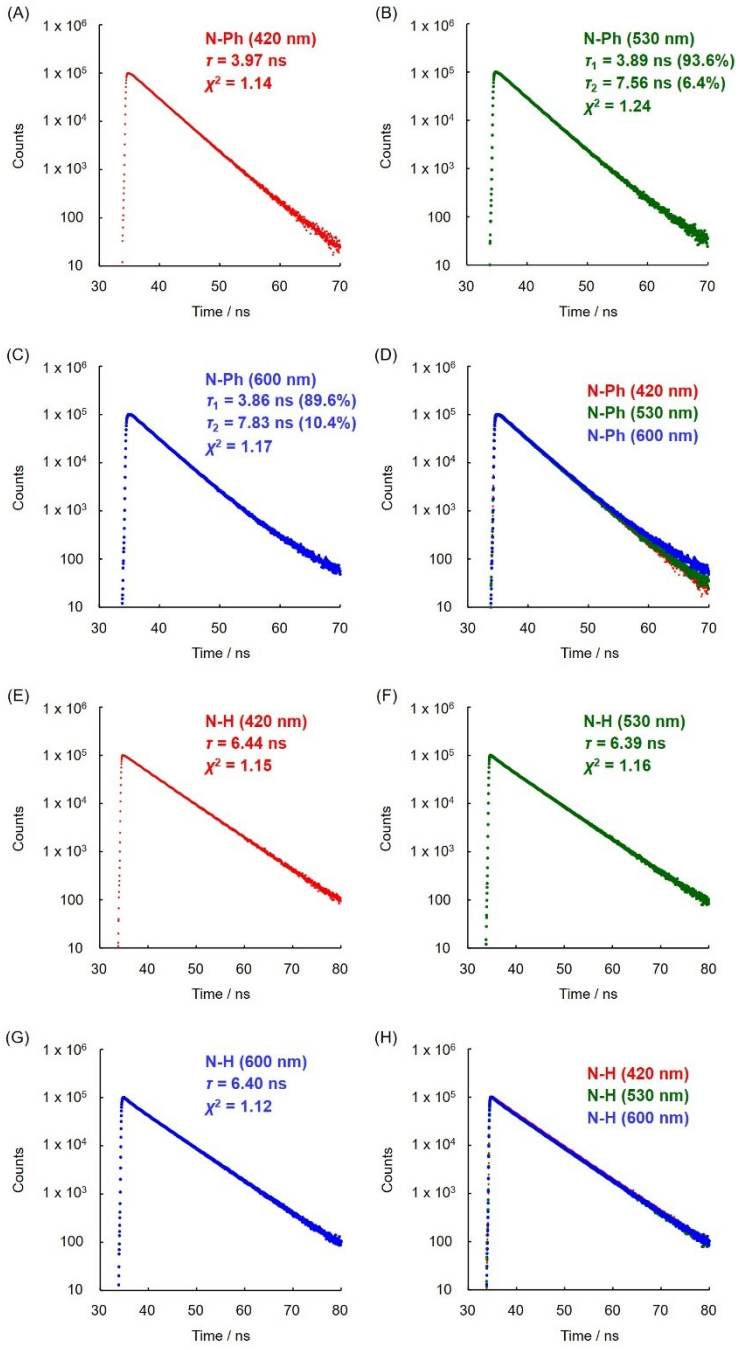

Figure S11. PL lifetime decay curves of **N-Ph** and **N-H** in CH_2Cl_2 (1.0×10^{-5} M) at room temperature, excited at 375 nm with LED laser. Estimated lifetimes were described in the figure. Monitored wavelengths were (A) and (E) 420 nm, (B) and (F) 530 nm, (C) and (G) 600 nm for **N-Ph** and **N-H**, respectively. (D), (H) Overwriting spectra of (A), (B), (C) and (E), (F), (G), respectively. In the case of **N-Ph**, the second and longer lifetime component was too weak to estimate the correct value. However, the difference depending on the monitoring wavelength was observed. In the case of **N-H**, the only single component was observed from various excited wavelengths.

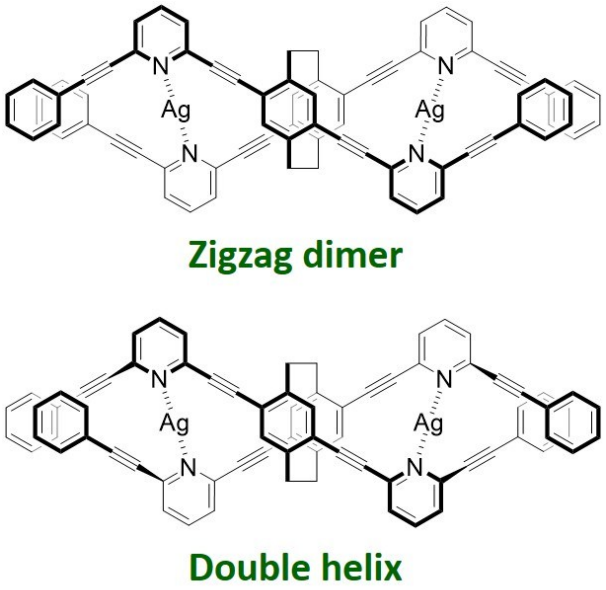

Figure S12. Predicted structures of (S_p)-**N-Ph-Ag**.

Computational details

The Gaussian 09 program package[4] was used for computation. We optimized the structures of the [(S_p)-**N-Ph-Ag**]$^{2+}$ in the ground S_0 states and calculated their structure energy. The density functional theory (DFT) was applied for the optimization of the structures in the S_0 states at the M06-2X/6-31g(d,p) for C, H, N and LANL2DZ for Ag levels. We calculated the structure energy in the ground S_0 states by DFT at the M06-2X/6-31g(d,p) for C, H, N and LANL2DZ for Ag levels.

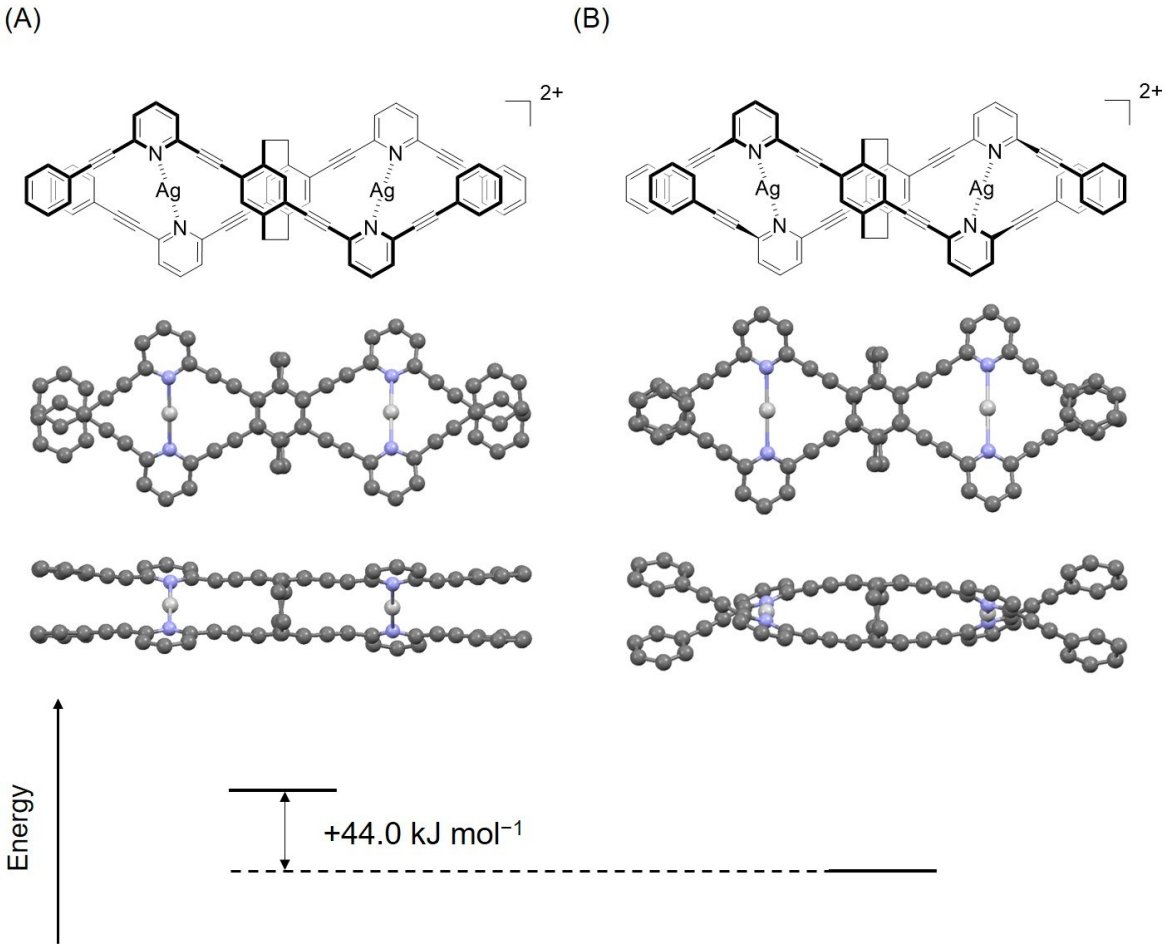

Figure S13. (A) Zigzag conformation and (B) double helical conformation of (S_p)-**Cp-N-Ph-Ag** by DFT with M06-2X/6-31G(d) for C, H, N and LANL2DZ for Ag//M06-2X/6-31G(d) for C, H, N and LANL2DZ for Ag levels.

Ag(I) titration measurement

Titration of AgOTf to (S_p) and (R_p)-**N-H** and **N-Ph** was carried out in dilute mixed CH_2Cl_2/DMF = 95:5 v/v solution (1.0×10^{-5} M). DMF was used for the preparation of AgOTf solution because CH_2Cl_2 is not good solvent for AgOTf. At first, (S_p)-**N-H**, **N-Ph** and AgOTf in dilute mixed CH_2Cl_2/DMF = 95:5 v/v solution (5.0×10^{-4} M) were prepared, respectively. Then, the AgOTf solution (from 0 mL to 0.50 mL) was titrated to the (S_p) and (R_p)-**N**, **N-Ph**, **N-Py** solution (0.10 mL) and made the total volume 5.0 mL (1.0×10^{-5} M) by pure CH_2Cl_2/DMF = 95:5 v/v solution. The titration spectra were shown here.

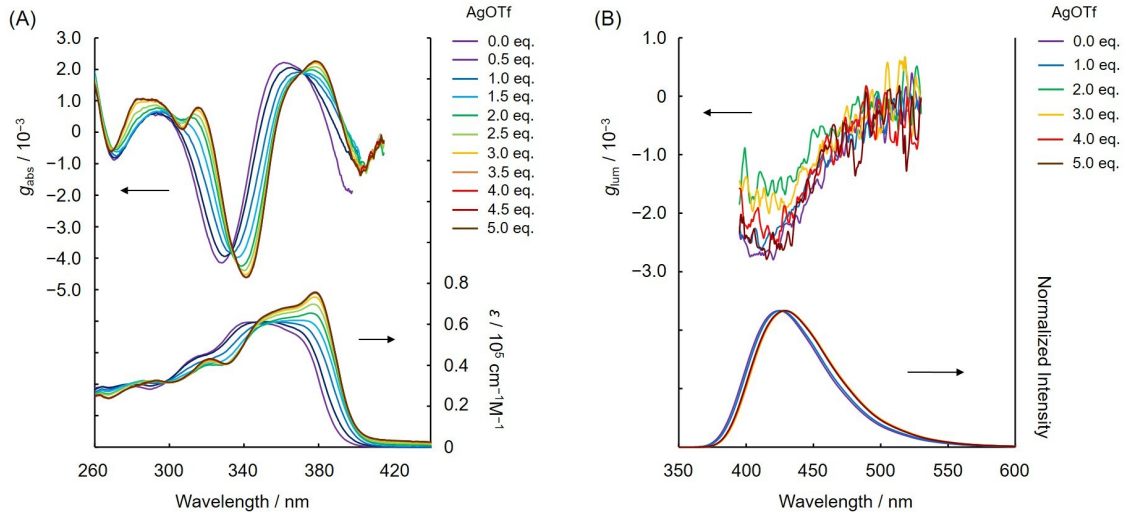

Figure S14. (A) CD (top) (g_{abs}) and UV–vis absorption (bottom) spectra and (B) CPL (top) (g_{lum}) and PL (bottom) spectra of AgOTf titration of (S_p)-**N-H** in dilute CH_2Cl_2/DMF = 95/5 v/v solution (1.0×10^{-5} M). Excitation wavelength was 300 nm.

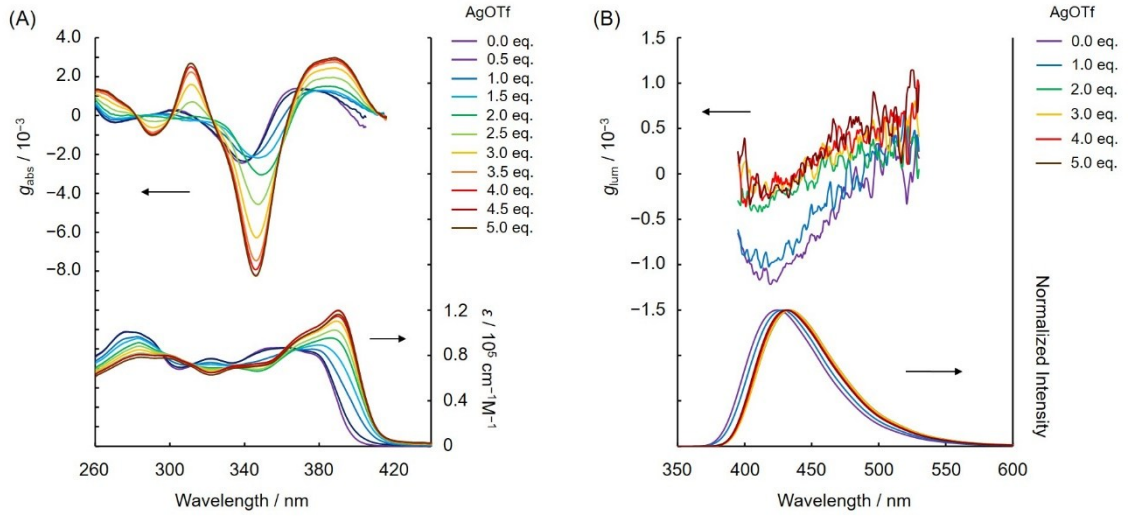

Figure S15. (A) CD (top) (g_{abs}) and UV–vis absorption (bottom) spectra and (B) CPL (top) (g_{lum}) and PL (bottom) spectra of AgOTf titration of (S_p)-**N-Ph** in dilute CH_2Cl_2/DMF = 95/5 v/v solution (1.0×10^{-5} M). Excitation wavelength was 300 nm.

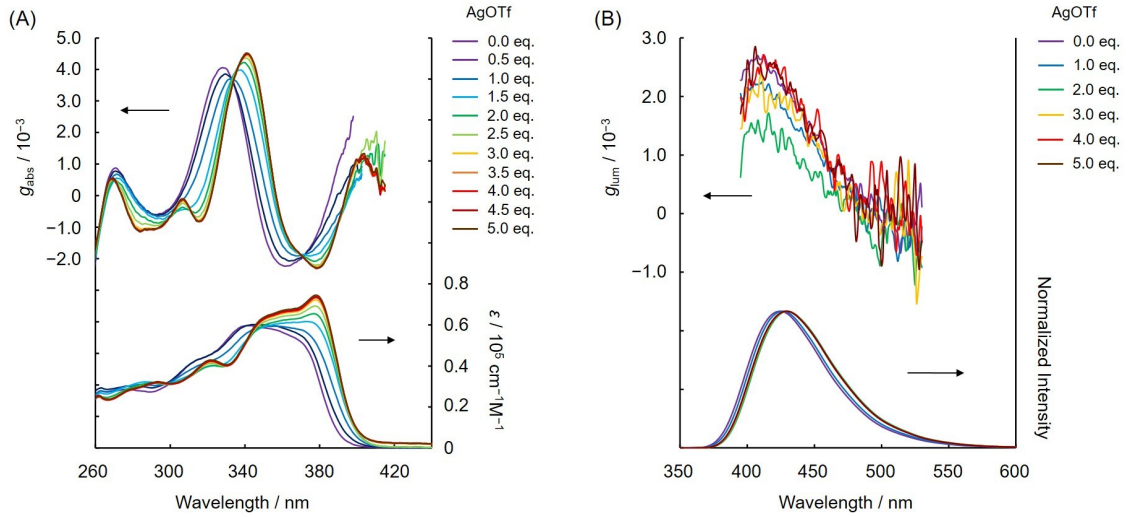

Figure S16. (A) CD (top) (g_{abs}) and UV–vis absorption (bottom) spectra and (B) CPL (top) (g_{lum}) and PL (bottom) spectra of AgOTf titration of (R_p)-**N-H** in dilute CH_2Cl_2/DMF = 95/5 v/v solution (1.0×10^{-5} M).

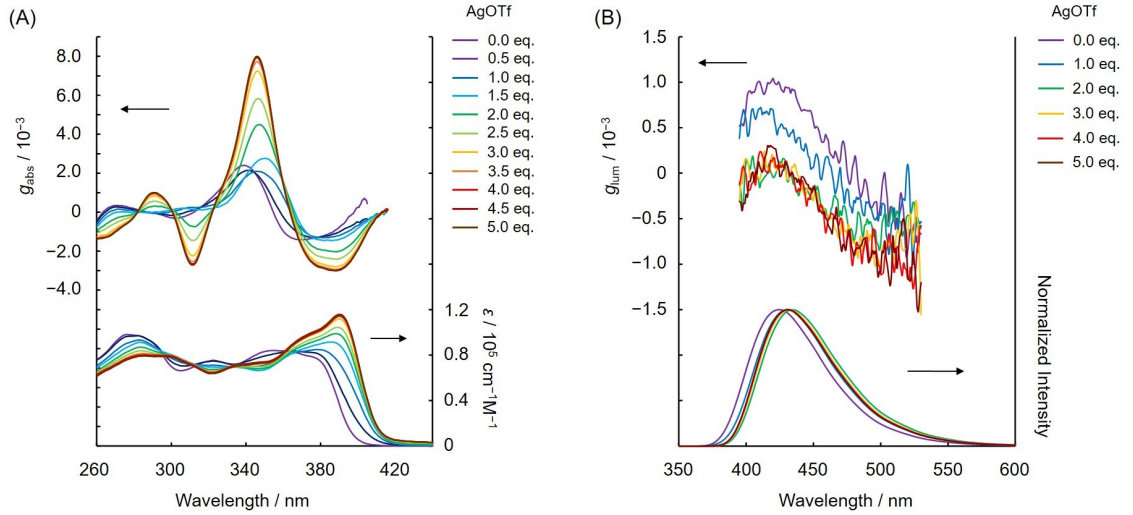

Figure S17. (A) CD (top) (g_{abs}) and UV–vis absorption (bottom) spectra and (B) CPL (top) (g_{lum}) and PL (bottom) spectra of AgOTf titration of (R_p)-**N-Ph** in dilute CH_2Cl_2/DMF = 95/5 v/v solution (1.0×10^{-5} M).

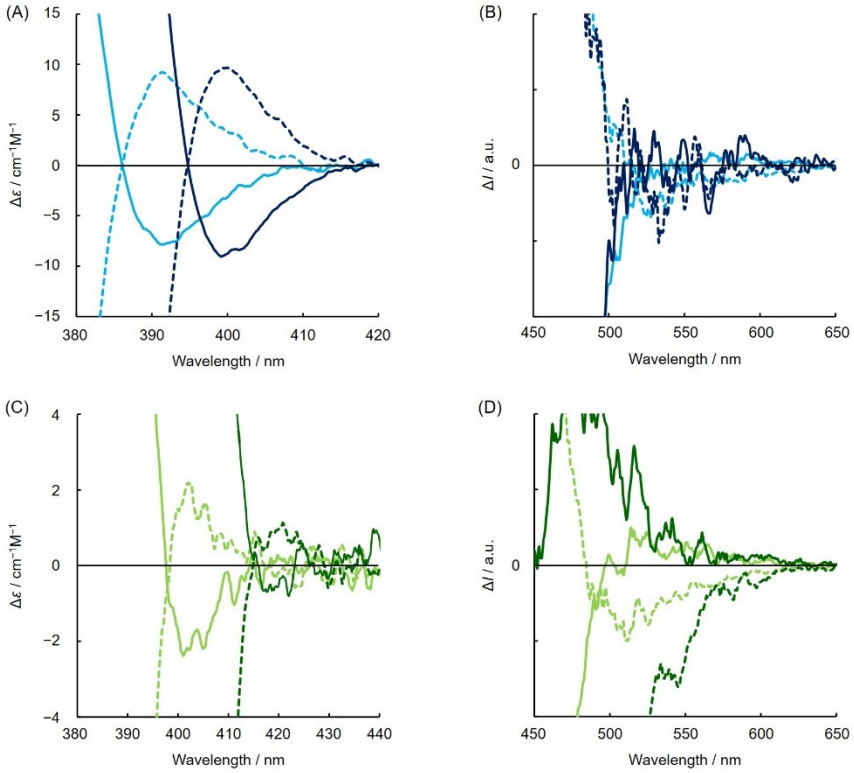

Figure S18. Expanded views of (A) CD and (B) CPL spectra of **N-H** and **N-H-Ag**, (C) CD and (D) CPL spectra of **N-Ph** and **N-Ph-Ag** in the dilute CH_2Cl_2 (1.0×10^{-5} M). Excitation wavelength was 300 nm.

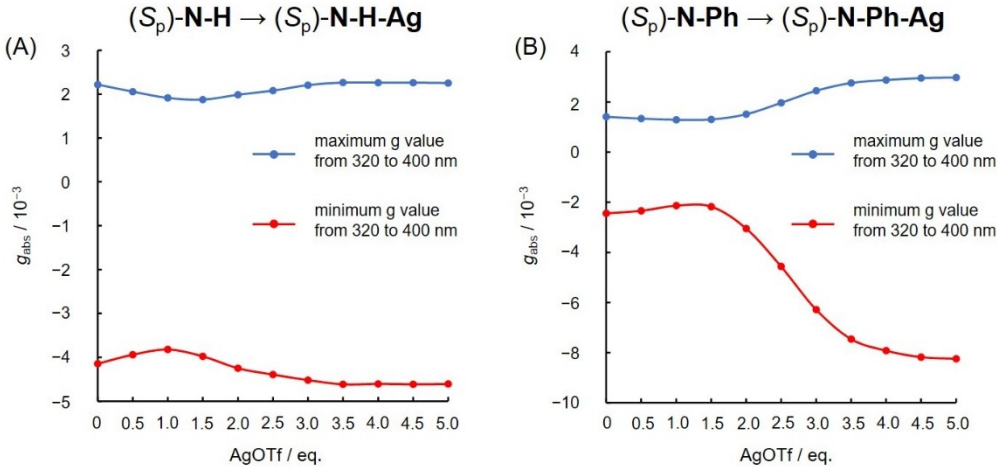

Figure S19. The values of g_{abs} during AgOTf titration to the (A) (S_p)-**N-H** and (B) (S_p)-**N-Ph** in dilute CH_2Cl_2/DMF = 95/5 v/v solution (1.0×10^{-5} M). Maximum (blue line) and minimum (red line) *g* values from 320 to 400 nm were monitored, respectively.

Single crystal X-ray structure analysis of *rac*-N-H

Intensity data were collected on a Rigaku R-AXIS RAPID imaging plate area detector with graphite monochromated MoKα radiation (λ = 0.71069 Å). The structures were solved and refined by full-matrix least-squares procedures based on F^2 (SHELX-2014).[5]

Table S2. Crystallographic data of *rac*-**N-H**

Empirical formula	$C_{44}H_{28}N_4$
Formula weight	612.70
Temperature (K)	93(2)
Wavelength (Å)	0.71075
Crystal system, space group	Triclinic, P-1
Unit cell dimensions	a=9.6882(6)
	b=13.1119(9)
	c=13.3082(8)
	α=108.885(8)
	β=94.201(7)
	γ=99.040(7)
Volume (Å^3)	1565.68(19)
Z, calculated density (Mg m^{-3})	2, 1.300
Absorption coefficient	0.077
F(000)	640
Crystal size (mm)	0.80 × 0.80 × 0.40
θ range for data collection	3.103-27.484
Limiting indices	$-11\le h\le 12$, $-17\le k\le 16$, $-16\le l\le 17$
Reflections collected (unique)	15348/7136 [R(int)=0.0352]
Completeness to theta	0.994
Max. and min. transmission	1.000, 0.3626
Goodness-of-fit on F^2	1.039
Final R indices [$I > 2\sigma(I)$][a]	R_1 = 0.0550, wR_2 = 0.1321
R indices (all data)	R_1 = 0.0783, wR_2 = 0.1473

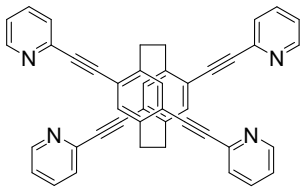

CCDC # 1548564

[a] $R_1 = \Sigma(|F_0|-|F_c|)/\Sigma|F_0|$. w$R_2 = [\Sigma w(F^2_0-F^2_c)^2/\Sigma w(F^2_0)^2]^{1/2}$. $w = 1/[\sigma^2(F^2_0)+[(ap)^2+bp]]$, where $p = [\max(F^2_0,0)+2F^2_c]/3$.

(A)

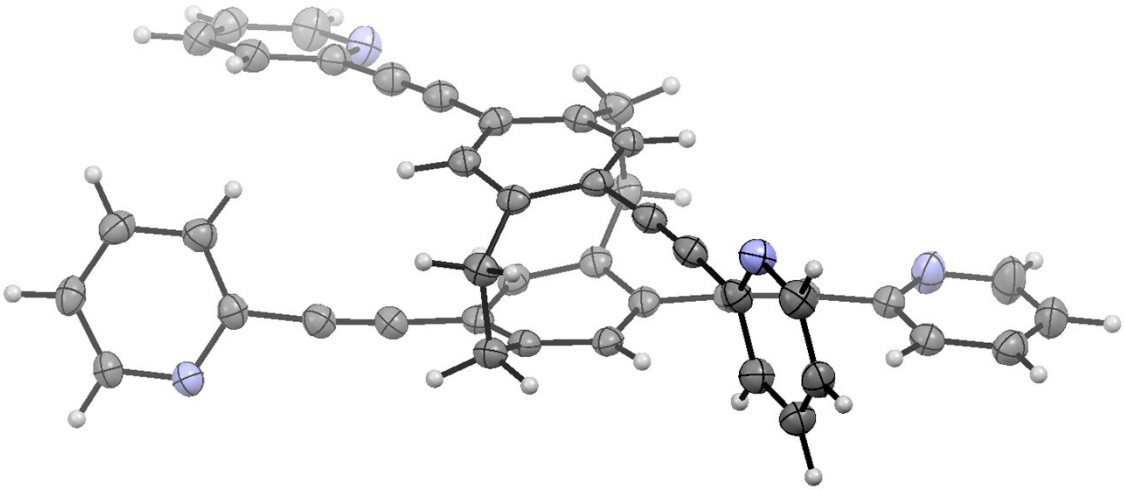

(B)

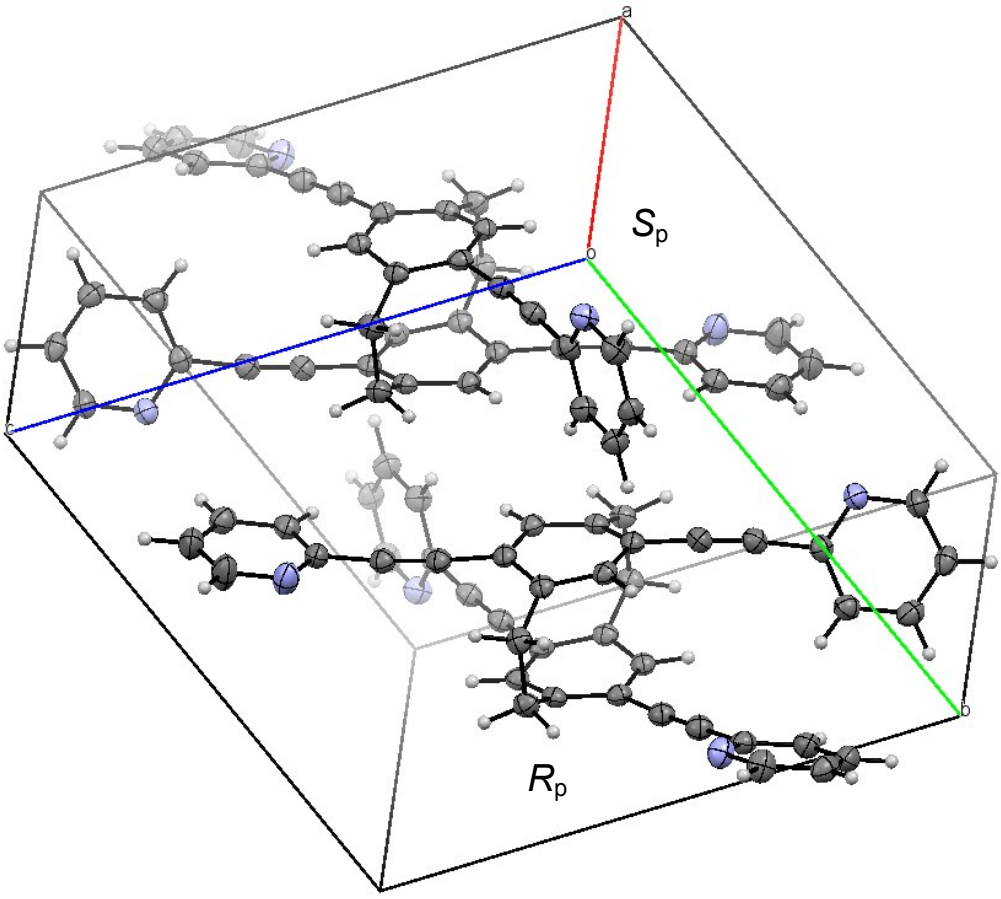

Figure S20. (A) ORTEP drawings of *rac*-**N-H** and (B) the packing diagram. Thermal ellipsoids are scaled to the 50% probability level.

Single crystal X-ray structure analysis of *rac*-N-H-Ag

Table S2. Crystallographic data of *rac*-**N-H-Ag**

Empirical formula	$C_{47}H_{30}N_4O_6F_6S_2Cl_2Ag_2$
Formula weight	1121.5
Temperature (K)	93(2)
Wavelength (Å)	0.71075
Crystal system, space group	Monoclinic, $P2_1/a$
Unit cell dimensions	a=14.8841(7)
	b=14.9687(7)
	c=21.4518(10)
	α=90
	β=102.663(7)
	γ=90
Volume (Å^3)	4663.1(4)
Z, calculated density (Mg m^{-3})	4, 1.726
Absorption coefficient	1.122
F(000)	2408.0
Crystal size (mm)	0.10 × 0.10 × 0.10
θ range for data collection	3.062-27.450
Limiting indices	$-17\leq h\leq 19$, $-19\leq k\leq 19$, $-27\leq l\leq 27$
Reflections collected (unique)	42967/10611 [R(int)=0.1672]
Completeness to theta	0.995
Max. and min. transmission	1.0000 and 0.3621
Goodness-of-fit on F^2	1.065
Final R indices [$I > 2\sigma(I)$][a]	R_1 = 0.0889, wR_2 = 0.1291
R indices (all data)	R_1 = 0.1674, wR_2 = 0.1516

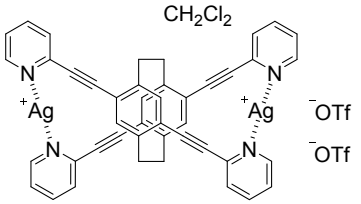

CCDC # 1548569

[a] $R_1 = \Sigma(|F_0|-|F_c|)/\Sigma|F_0|$. w$R_2 = [\Sigma w(F^2_0-F^2_c)^2/\Sigma w(F^2_0)^2]^{1/2}$. $w = 1/[\sigma^2(F^2_0)+[(ap)^2+bp]]$, where $p = [\max(F^2_0,0)+2F^2_c]/3$.

(A)

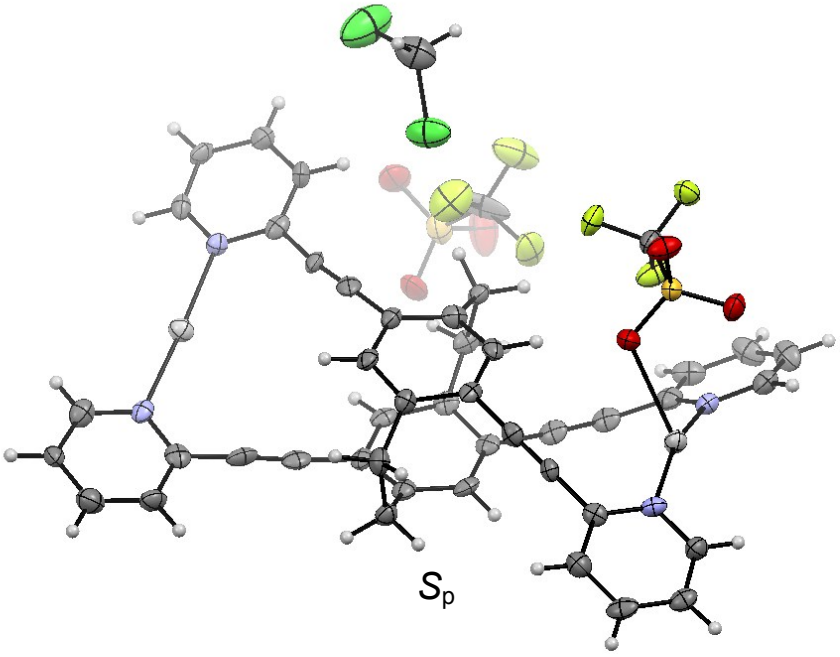

(B)

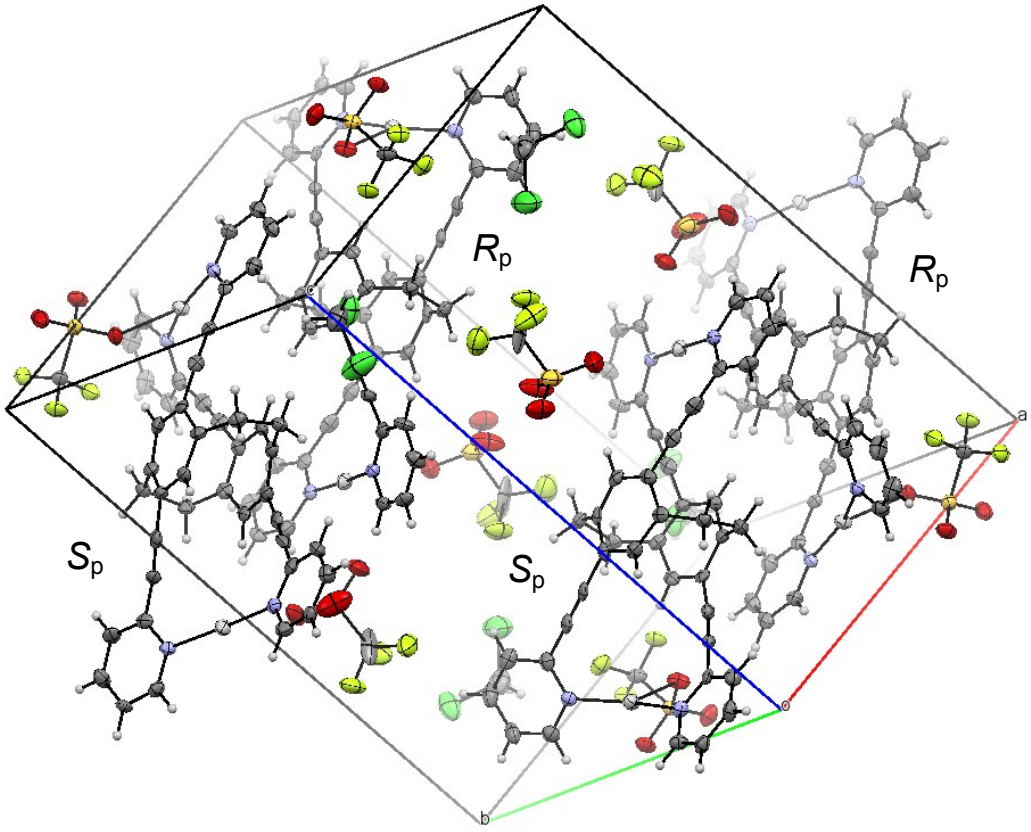

Figure S21. (A) ORTEP drawings of *rac*-**N-H-Ag** with CH_2Cl_2 and (B) the packing diagram. Thermal ellipsoids are scaled to the 50% probability level.

References

1. A. B. Pangborn, M. A. Giardello, R. H. Grubbs, R. K. Rosen and F. J. Timmers, *Organometallics* 1996, **15**, 1518–1520.

2. Q. Li, F. Huang, Y. Fan, Y. Wang, J. Li, Y. He and H. Jiang, *Eur. J. Inorg. Chem.* 2014, **20**, 3235–3244.

3. Y. Morisaki, M. Gon, T. Sasamori, N. Tokitoh and Y. Chujo, *J. Am. Chem. Soc.* 2014, **136**, 3350–3353.

4. Gaussian 09, Revision D.01, M. J. Frisch, G. W. Trucks, H. B. Schlegel, G. E. Scuseria, M. A. Robb, J. R. Cheeseman, G. Scalmani, V. Barone, B. Mennucci, G. A. Petersson, H. Nakatsuji, M. Caricato, X. Li, H. P. Hratchian, A. F. Izmaylov, J. Bloino, G. Zheng, J. L. Sonnenberg, M. Hada, M. Ehara, K. Toyota, R. Fukuda, J. Hasegawa, M. Ishida, T. Nakajima, Y. Honda, O. Kitao, H. Nakai, T. Vreven, Jr., J. A. Montgomery, J. E. Peralta, F. Ogliaro, M. Bearpark, J. J. Heyd, E. Brothers, K. N. Kudin, V. N. Staroverov, R. Kobayashi, J. Normand, K. Raghavachari, A. Rendell, J. C. S. Burant, S. Iyengar, J. Tomasi, M. Cossi, N. Rega, J. M. Millam, M. Klene, J. E. Knox, J. B. Cross, V. Bakken, C. Adamo, J. Jaramillo, R. Gomperts, R. E. Stratmann, O. Yazyev, A. J. Austin, R. Cammi, C. Pomelli, J. W. Ochterski, R. L. Martin, K. Morokuma, V. G. Zakrzewski, G. A. Voth, P. Salvador, J. J. Dannenberg, S. Dapprich, A. D. Daniels, Ö. Farkas, J. B. Foresman, J. V. Ortiz, J. Cioslowski and D. J. Fox, Gaussian, Inc., Wallingford CT, 2009.

5. Sheldrick, G. M. *Acta Cryst.* 2008, **A64**, 112–122.